

# Lawrence Berkeley National Laboratory

## LBL Publications

### Title

OPTICAL STUDY AND ANALYSIS OF  $\text{Pu}^{4+}$  IN SINGLE CRYSTALS OF  $\text{ZrSiO}_4$ .

### Permalink

<https://escholarship.org/uc/item/5km222xr>

### Authors

Poirot, I.S.

Kot, W.K.

Edelstein, N.M.

### Publication Date

1988-08-01

c.2



# Lawrence Berkeley Laboratory

UNIVERSITY OF CALIFORNIA

## Materials & Chemical Sciences Division

Submitted to Physical Review B

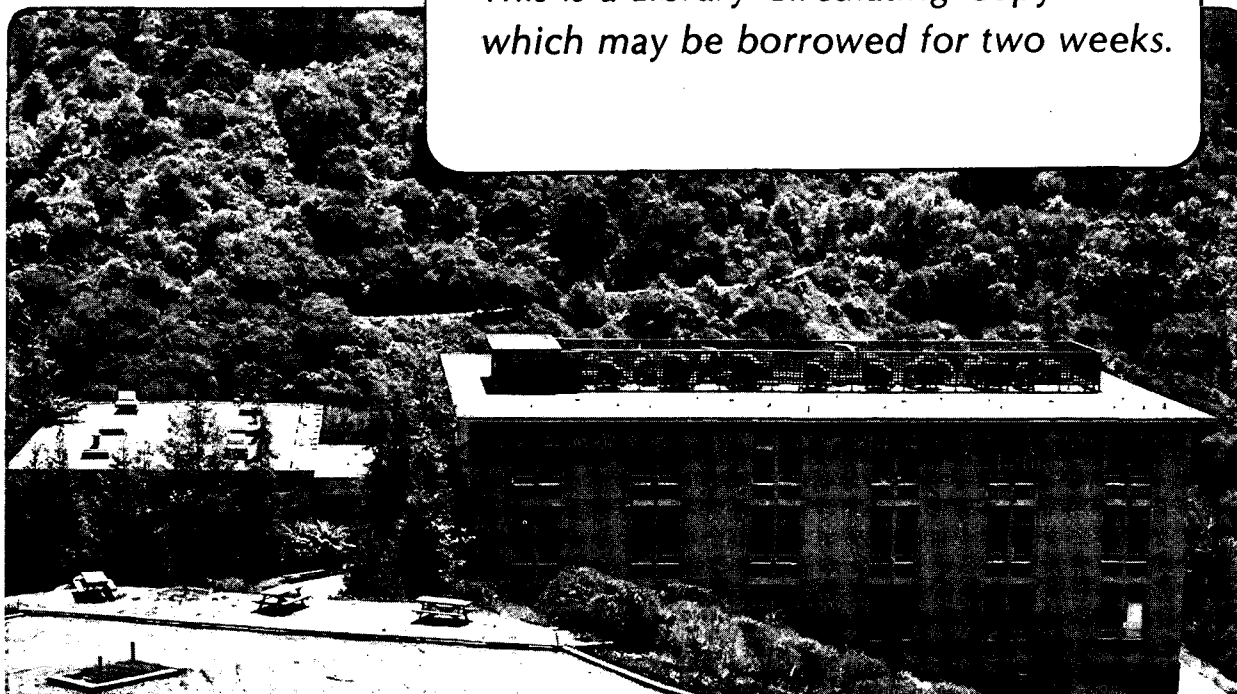
### Optical Study and Analysis of $\text{Pu}^{4+}$ in Single Crystals of $\text{ZrSiO}_4$

I.S. Poirot, W.K. Kot, N.M. Edelstein,  
M.M. Abraham, C.B. Finch, and L.A. Boatner

August 1988

**TWO-WEEK LOAN COPY**

*This is a Library Circulating Copy  
which may be borrowed for two weeks.*



LBL-25729  
c.2

## **DISCLAIMER**

This document was prepared as an account of work sponsored by the United States Government. While this document is believed to contain correct information, neither the United States Government nor any agency thereof, nor the Regents of the University of California, nor any of their employees, makes any warranty, express or implied, or assumes any legal responsibility for the accuracy, completeness, or usefulness of any information, apparatus, product, or process disclosed, or represents that its use would not infringe privately owned rights. Reference herein to any specific commercial product, process, or service by its trade name, trademark, manufacturer, or otherwise, does not necessarily constitute or imply its endorsement, recommendation, or favoring by the United States Government or any agency thereof, or the Regents of the University of California. The views and opinions of authors expressed herein do not necessarily state or reflect those of the United States Government or any agency thereof or the Regents of the University of California.

LBL-25729

Optical Study and Analysis of  $\text{Pu}^{4+}$  in Single Crystals of  $\text{ZrSiO}_4$

I.S. Poirot, W.K. Kot, N.M. Edelstein  
Department of Chemistry, University of California  
and  
Materials and Chemical Sciences Division  
Lawrence Berkeley Laboratory, 1 Cyclotron Road  
Berkeley, California 94720

and

M.M. Abraham, C.B. Finch, L.A. Boatner  
Solid State Division  
Oak Ridge National Laboratory  
Oak Ridge, Tennessee 37831

ABSTRACT

The electronic structure of tetravalent plutonium incorporated as a dilute impurity in single crystals of the tetragonal host  $\text{ZrSiO}_4$  has been studied using polarized optical spectroscopy. Fifty-three crystal-field levels were assigned and used to obtain a fit to a parametric Hamiltonian to within an rms deviation of  $33 \text{ cm}^{-1}$ . The resulting crystal field parameters were similar to those obtained for the  $\text{ZrSiO}_4:\text{U}^{4+}$  and  $\text{ZrSiO}_4:\text{Np}^{4+}$  systems. The parametric fit improves with increasing atomic number across the actinide series, suggesting that the tetravalent actinides are more "lanthanide like" as the atomic number increases.

## Introduction

Optical spectroscopic investigations of the narrow absorption and fluorescence spectra of trivalent lanthanide and actinide ions in various host single crystals have been studied for over 30 years. The parametric theory used to interpret these spectra has been quite successful for these ionic systems and, in particular, it has proven to be very useful when applied to the lanthanides.<sup>1</sup> The same theory applied to tetravalent actinide ions such as  $U^{4+}$ , however, results in fits to the experimental spectra that are much worse than those found for the trivalent ions.<sup>2</sup> At the present time, these findings are based on only a relatively small number of experimental studies of tetravalent ions with atomic number  $Z$  greater than 92 due, in part, to the problems associated with the radioactivity of these elements. Since the heavier actinide ions become more lanthanide-like in their electronic properties because of the contraction of the 5f orbitals, one would expect the conventional parametric theory to be more successful when applied to the higher  $Z$  tetravalent actinides. Accordingly, the present work represents one portion of a systematic study of the higher  $Z$  tetravalent actinide ions diluted as impurities in various host single crystals.

The optical spectrum of  $ZrSiO_4:U^{4+}$  has been extensively investigated,<sup>3</sup> and we have recently published an optical and electron paramagnetic resonance study of tetravalent neptunium in single crystal  $ZrSiO_4$ .<sup>4</sup> The present work represents the results of an investigation of the optical spectrum of  $Pu^{4+}$  doped into single crystals of  $ZrSiO_4$  and a parametric analysis of these data. In carrying out this analysis, it has been assumed that the crystal-field parameters obtained for

$\text{ZrSiO}_4:\text{Np}^{4+}$  represent reasonable initial values for the  $\text{ZrSiO}_4:\text{Pu}^{4+}$  case, since Np and Pu are neighboring elements in the periodic table.

### Experimental

Single crystals of  $\text{ZrSiO}_4$  doped with approximately 0.2 wt. %  $^{242}\text{Pu}$  were grown as described previously.<sup>5-7</sup> Crystals selected for the optical measurements had dimensions on the order of  $2 \times 2 \times 2 \text{ mm}^3$  with well-formed faces and were purple in color. The crystal to be examined was mounted on a slotted copper plate with the optical axis either parallel or perpendicular to the slot. The crystal and plate were then mounted and sealed into a quartz tube containing ~ 200 mm Hg of He gas.

The optical absorption spectra in both the  $\sigma$ - and the  $\pi$ -polarizations were obtained between 2200 nm and 400 nm at 77K and 4.2K using a Cary model 17 spectrophotometer. Absorption spectra in the 760-390 nm range were recorded at 4.2K with Jarrell-Ash F6 and 3.4 m-spectrographs.

The observed line widths were relatively broad ( $15\text{-}200 \text{ cm}^{-1}$ ), with an average width of about  $35 \text{ cm}^{-1}$ , even at low temperatures. This was especially true for the high-energy peaks. No attempt was made to measure the Zeeman splittings, since the calculated g values are generally small for the doubly degenerate  $\Gamma_5$  states and the line widths are relatively broad.

### Preliminary Calculations

Single crystals of  $\text{ZrSiO}_4$  (zircon) are tetragonal with the tetravalent metal ion located at a  $D_{2d}$  symmetry site. The  $\text{Zr}^{4+}$  ion is

surrounded by eight oxygen atoms in a dodecahedral array with the  $S_4$  axis parallel to the optic axis of the crystal.<sup>8,9</sup> A  $\text{Pu}^{4+}$  ion substitutes for a  $\text{Zr}^{4+}$  ion in the doped crystals. In  $D_{2d}$  symmetry, the J states of an  $f^n$  ion (n even) decompose into five different representations: four singlets,  $\Gamma_1$  through  $\Gamma_4$ , and one doubly-degenerate  $\Gamma_5$  representation. The selection rules for  $D_{2d}$  symmetry are shown in Table I.

The energy levels within an  $f^n$  configuration in  $D_{2d}$  symmetry can be obtained by diagonalizing the matrix elements of the free-ion ( $H_{\text{FI}}$ ) and crystal-field ( $H_{\text{CF}}$ ) Hamiltonians:<sup>10-12</sup>

$$\begin{aligned}
 H_{\text{FI}} = & \sum_{k=0,2,4,6} F^k(\text{nf}, \text{nf}) f_k + \zeta_f a_{\text{s.o.}} + \alpha L(L+1) \\
 & + \beta G(G_2) + \gamma (R_7) + \sum_{\substack{k=2-8 \\ k \neq 5}} T^k t_k \\
 & + \sum_{k=0,2,4} M^k m_k + \sum_{k=2,4,6} P^k p_k, \quad (1)
 \end{aligned}$$

and

$$\begin{aligned}
 H_{\text{CF}} = & B_0^2 C_0^2 + B_0^4 C_0^4 + B_4^4 (C_4^4 + C_{-4}^4) \\
 & + B_0^6 C_0^6 + B_4^6 (C_4^6 + C_{-4}^6). \quad (2)
 \end{aligned}$$

The  $F^k(\text{nf}, \text{nf})$ 's and  $\zeta_f$  above represent the radial parts of the electrostatic and spin-orbit interactions, respectively, between f electrons, while  $f_k$ 's and  $a_{\text{s.o.}}$  are angular parts of these interactions.

The parameters  $\alpha$ ,  $\beta$ , and  $\gamma$  are associated with the two-body effective operators of the configuration interaction and the  $T^k$ 's are the corresponding parameters of the three-body configuration interaction operators. The  $M^k$  parameters represent the spin-spin and spin-other-orbit interactions, while the  $P^k$  parameters arise from electrostatic-spin-orbit interactions with higher configurations. The crystal-field interaction for  $D_{2d}$  symmetry is parametrized by  $B_0^2$ ,  $B_0^4$ ,  $B_4^4$ ,  $B_0^6$ , and  $B_4^6$ , and the angular operators  $C_q^{(k)}$  are the usual Racah tensors.

For the  $f^4$  configuration ( $D_{2d}$  symmetry), the matrix elements were factored by the crystal quantum number  $\mu$  into  $\mu = 0, \pm 1, 2$  matrices with the  $\mu = \pm 1$  matrix being doubly degenerate and corresponding to the  $\Gamma_5$  representation. The  $\mu=0$  and  $\mu=2$  matrices could be further decomposed into representations  $\Gamma_1$ ,  $\Gamma_2$  and  $\Gamma_3$ ,  $\Gamma_4$  respectively, but this was not done.<sup>13</sup> The calculations were carried out using non-truncated matrices for the  $f^4$  configuration with ranks ranging from 245 to 257.

A preliminary calculation was performed using the free-ion parameters taken from the analyses of Blaise<sup>14</sup> and Carnall<sup>15</sup> and the  $ZrSiO_4:Np^{4+}$  crystal-field parameters.<sup>4</sup> This calculation showed the lowest energy term is primarily a  $^5I_4$  multiplet which splits into a  $\Gamma_3$  ground state with a  $\Gamma_5$  first excited state located at approximately  $500 \text{ cm}^{-1}$ . It was assumed that this approach gave the correct ordering of the levels and the results were used as a guide for the energy level assignments.



### Results and Assignments of Levels

Wavelengths, intensities, and polarization characteristics of the optical transitions are presented in Table II together with their assignments. As noted in earlier work for  $U^{4+}$  and  $Np^{4+}$  in  $ZrSiO_4$ ,<sup>3,4</sup> more lines were observed than predicted from the calculated spectrum, with many of the lines being rather weak. These extra lines could not be consistently assigned as vibronic transitions. All of the strong lines that could be assigned were taken as zero-phonon transitions. The extra lines were strongly polarized and may be due to the presence of different symmetry sites and/or to  $Pu^{3+}$ .

Three lines were observed in the room temperature spectrum that disappeared at low temperatures. These lines occurred at  $4608\text{ cm}^{-1}$  ( $\sigma$ ),  $8452\text{ cm}^{-1}$  ( $\pi$ ), and  $10740\text{ cm}^{-1}$  ( $\sigma$ ) and were assigned as transitions from the  $\Gamma_5$  ( $522\text{ cm}^{-1}$ ) level to  $\Gamma_2$ ,  $\Gamma_5$ , and  $\Gamma_2$  levels respectively. Transitions from the  $\Gamma_3$  ground state to these three states with energies at  $5129\text{ cm}^{-1}$  ( $\pi\ \Gamma_2$ ),  $8974\text{ cm}^{-1}$  ( $\sigma\ \Gamma_5$ ) and  $11262\text{ cm}^{-1}$  ( $\pi\ \Gamma_2$ ) were also observed. A line structure of this type could theoretically be observed with a different symmetry ground state; however, it could not be fitted to give a consistent set of parameters. If a doublet  $\Gamma_5$  state were lowest, then many more lines would have been observed (see Table I). The room temperature spectrum was also indicative of the presence of another excited state at  $756\text{ cm}^{-1}$ ; and a  $\Gamma_1$  and a  $\Gamma_2$  state were calculated to lie at  $706\text{ cm}^{-1}$  and  $782\text{ cm}^{-1}$ , respectively. These assignments, however, could not be verified. Two additional peaks that were only detected at room temperature also could not be assigned.

In the 4600 to 6600  $\text{cm}^{-1}$  region, two very strong  $\pi$ -lines and four strong to medium  $\sigma$ -lines were observed in agreement with the two  $\pi$ -lines and three  $\sigma$ -lines predicted by the calculation based on a  $\Gamma_3$  ground state. For any other singlet ground state, only one zero-phonon  $\pi$ -line would be present. The three strongest  $\sigma$ -lines were assigned as transitions to different  $\Gamma_5$  states. The fourth  $\sigma$ -line at 5467  $\text{cm}^{-1}$  could be assigned to  $\text{Pu}^{3+}$  as shown by comparison with the spectrum of  $\text{LuPO}_4:\text{Pu}^{3+}$ .<sup>16</sup>

In the second group of peaks in the 8450 to 10100  $\text{cm}^{-1}$  region, again more lines were observed than calculated. Three  $\sigma$ -lines and one  $\pi$ -line were expected. In the  $\sigma$ -spectra, the weak lines at 8731, 8769, 8816, 8966, and 9176  $\text{cm}^{-1}$  could all be attributed to  $\text{Pu}^{3+}$  since the same pattern of lines was also present for  $\text{LuPO}_4:\text{Pu}^{3+}$ , but with the spectrum shifted by 300 - 400  $\text{cm}^{-1}$  toward the low energy side.<sup>16</sup> Three  $\Gamma_5$  states were then assigned. In the  $\pi$ -spectrum, one very strong peak plus eight weaker peaks were present. The  $\Gamma_2$  state was assigned to the strongest line which was two orders of magnitude stronger than the other lines. Three strong  $\pi$ -lines were predicted for any singlet ground state other than a  $\Gamma_3$ .

The next group of lines from 11000  $\text{cm}^{-1}$  to 16200  $\text{cm}^{-1}$  represent levels derived from eight different free-ion multiplets. The crystal-field levels overlapped to such an extent that no energy gap was seen within the group. All but one of the strong-to-medium peaks could be assigned based on their polarization characteristics. In all, 20 levels, (7  $\Gamma_2$  and 13  $\Gamma_5$ ), were assigned as compared to the 25 lines predicted by the calculation (8  $\Gamma_2$  and 17  $\Gamma_5$ ).

The highest energy portion of the spectrum (17200 to 25200  $\text{cm}^{-1}$ ) consisted of peaks that were much weaker and broader than the other groups. Some of these peaks had line widths of over 200  $\text{cm}^{-1}$  and, although they exhibited good polarization characteristics, they were not assigned, since an accurate determination of the peak positions was difficult. Twenty-one crystal-field states (9  $\Gamma_2$  and 12  $\Gamma_5$ ) were assigned based on the calculation leaving 6  $\Gamma_2$  and 17  $\Gamma_5$  states unassigned.

#### Parametric Fit of the Optical Data

The free-ion parameters were first varied with the crystal-field parameters fixed at the  $\text{ZrSiO}_4:\text{Np}^{4+}$  values.<sup>4</sup> In subsequent fits, the free-ion parameters  $F^2$ ,  $F^4$ ,  $F^6$ ,  $\zeta$ ,  $\alpha$ ,  $\beta$  and all of the crystal-field parameters were allowed to vary simultaneously;  $\gamma$ ,  $T^2$ ,  $M^0$  and  $P^2$  were also varied with the ratios  $M^0/M^2$ ,  $M^0/M^4$ ,  $P^2/P^4$  and  $P^2/P^6$  fixed. A total of 53 levels was assigned and fitted with an rms deviation of 33  $\text{cm}^{-1}$ . Two sets of calculated parameters, (A) with  $\gamma$ ,  $T^2$ ,  $M^0$ ,  $P^2$  fixed and (B) with  $\gamma$ ,  $T^2$ ,  $M^0$ ,  $P^2$  varied, are presented in Table III for the purpose of comparison. When allowed to vary,  $\gamma$ ,  $M^0$ ,  $T^2$ , and  $P^2$  all increased substantially but with a corresponding decrease of the  $F^k$  integrals, reflecting the fact that a number of these parameters are not orthogonal.<sup>17</sup> In general the rms deviation  $\sigma$  showed a significant improvement while the crystal-field parameters only changed slightly when the parameters  $\gamma$ ,  $M^0$ ,  $T^2$  and  $P^2$  were varied. It should be noted, however, that the  $M^0$  value obtained was much greater than the relativistic Hartree-Fock value. Both sets of fits produced essentially

the same energy ordering of the crystal-field levels with only relatively few interchanges occurring. For the sake of consistency in making comparisons with the other systems, the parameter set A is used in the discussion section that follows.

A parametric fit using 17 of the strongest spectral lines with good polarization characteristics was also performed ( $\sigma = 27 \text{ cm}^{-1}$ ), and the parameters thus obtained were very similar to those reported above. The one exception was  $B_0^4$  which had a value of  $3200 \text{ cm}^{-1}$ , about 12% larger than the values shown in Table III. This is reassuring since it is possible that some of the weaker lines were incorrectly assigned and could be due to  $\text{Pu}^{3+}$ . Most of the weak lines, however, were not assigned.

A table of calculated and experimental energies plus the two leading terms in the wavefunction for each energy level is given in the Supplementary Material.

### Discussion

Despite the large crystal-field splittings of  $\text{Pu}^{4+}$  in a  $\text{ZrSiO}_4$  single crystal, the similarity between the present spectrum and that of  $\text{Pu}^{4+}$  in solution is clearly evident. This similarity has already been noted in other studies involving compounds of higher symmetry, such as  $\text{K}_2\text{PuCl}_6$  and  $\text{Rb}_2\text{PuCl}_6$ .<sup>18</sup> A parametric analysis has not been performed in those cases, however, and an inclusion of the crystal-field interaction in the present calculation of the energy levels resulted in free-ion parameters that are quite different from the predicted ones. Crosswhite and others have found it useful to compare the differences

between experimentally-determined parameters and those calculated using Hartree-Fock methods with relativistic corrections.<sup>14,19,20</sup> The differences vary smoothly across the series in  $\text{LaCl}_3:\text{Ln}^{3+}$  and  $\text{LaCl}_3:\text{An}^{3+}$  and are useful for predicting free-ion parameters. Table IV lists the Hamiltonian parameters for  $\text{U}^{4+}$ ,  $\text{Np}^{4+}$ , and  $\text{Pu}^{4+}$  all doped into  $\text{ZrSiO}_4$ . Table V lists the differences between the relativistic Hartree-Fock and the experimental free ion parameters for the  $\text{ZrSiO}_4:\text{An}^{4+}$  series. The differences for  $F^2$  are almost constant, but the differences for  $F^4$ ,  $F^6$ , and  $\zeta$  do not show any trends. The ratios  $F_{\text{cry}}^2/F_{\text{fi}}^2$  and  $F_{\text{cry}}^4/F_{\text{cry}}^2$ , however, do agree with the expected decrease of covalency across the series.<sup>4</sup> Fixing the parameters at the predicted values resulted in much poorer fits ( $\sigma > 60 \text{ cm}^{-1}$ , with many inversions of experimental levels), and the fits did not converge. Varying the parameters with the initial input set at the predicted values only produced values similar to those reported here. However, the free-ion Slater integrals were obtained over a small energy range, (energy levels were assigned only up to  $-25,000 \text{ cm}^{-1}$ ) and future improvement is likely. The usefulness of the predictive model as applied to the tetravalent actinides has yet to be established.

The crystal-field parameters obtained for  $\text{ZrSiO}_4:\text{Pu}^{4+}$  are found to be very similar to those for  $\text{ZrSiO}_4:\text{U}^{4+}$  and  $\text{ZrSiO}_4:\text{Np}^{4+}$ , as indicated by the Auzel parameters  $[N_{\text{v}}/(4\pi)^{1/2}]$  in Table IV.<sup>21</sup> Trivalent actinides doped into  $\text{LaCl}_3$  also exhibit very similar crystal-field parameters within the series. It is seen from Table IV that the general quality of the fit improves across the actinide series. This may be due to the smaller ionic size of  $\text{Pu}^{4+}$  which is expected to cause the lowest

distortion of the surrounding ions and/or to the fact that the 5f electronic shell is more contracted (more lanthanide-like) for the higher atomic number. It should also be noted that the  $5f^{N-1}6d$  configuration shifts to higher energies as the atomic number increases.

### Conclusions

The optical spectrum of  $ZrSiO_4:Pu^{4+}$  has been analysed and fitted to a parametrized Hamiltonian. Relatively good fits were obtained, and two sets of parameters exhibiting the smallest rms deviations between the experimental and calculated levels are presented. Varying the parameters  $\gamma$ ,  $T^2$ ,  $M^0$  and  $P^0$  slightly improves the fits and changes the free-ion Slater parameters. The free-ion Slater integrals do not agree well with those computed by a predictive model, and no discernable trend is observed for the crystal-field parameters obtained for the series  $U^{4+}$ ,  $Np^{4+}$ , and  $Pu^{4+}$ . The general improved quality in the fits, however, indicates that the tetravalent actinide ions are more "lanthanide-like" as the atomic number increases.

### Acknowledgement

This work was supported by the Director, Office of Energy Research, Office of Basic Energy Sciences, Chemical Sciences Division of the U.S. Department of Energy under Contract No. DE-AC03-76SF00098 and by the Division of Materials Science, U.S. Department of Energy, under Contract No. DE-AC05-84OR21400 with Martin Marietta Energy System, Inc.

## References

- [1] J. P. Hessler and W. T. Carnall in "Lanthanide and Actinide Chemistry and Spectroscopy," (ACS Symp. Ser. no. 131), edited by N. Edelstein, (American Chemical Society, Washington, D.C., 1980), p.349.
- [2] N. Edelstein, *J. Less-Common Met.* 133, 39 (1987.); C. D. Flint and P. A. Tanner, *Mol. Phys.* 61, 389 (1987).
- [3] D. J. Mackey, W. A. Runciman, and E. R. Vance, *Phys. Rev. B* 11, 211 (1975).
- [4] I. Poirot, W. Kot, G. Shalimoff, N. Edelstein, M. M. Abraham, C. B. Finch and L. A. Boatner, *Phys. Rev. B* 37, 3255 (1988).
- [5] A. A. Ballman and R. A. Laudise, *J. Amer. Ceram. Soc.* 48, 130 (1965).
- [6] A. B. Chase and J. A. Osmer, *J. Electrochem. Soc.* 113, 198 (1966).
- [7] D. Ball and B. M. Wanklyn, *Phys. Status Solidi A* 36, 307 (1976).
- [8] R. W. Wyckoff, "Crystal Structures," 2nd Ed. (Interscience, New York, 1965), Vol.3, p. 15.
- [9] R. W. Reynolds, L. A. Boatner, C. B. Finch, A. Chatelain and M. M. Abraham, *J. Chem. Phys.* 56, 5607 (1972).
- [10] B. G. Wybourne, "Spectroscopic Properties of the Rare Earths," (Wiley, New York, 1965).
- [11] B. R. Judd, "Operator Techniques in Atomic Spectroscopy," (McGraw-Hill, New York, 1963).



- [12] W. T. Carnall, H. Crosswhite, H. M. Crosswhite, J. P. Hessler, N. M. Edelstein, J.G. Conway, G. V. Shalimoff and R. Sarup, J. Chem. Phys. 72, 5089 (1980).
- [13] See for example, chapter 6 in reference 10.
- [14] J. Blaise, M. S. Fred, W. T. Carnall, H. M. Crosswhite and H. Crosswhite in "Plutonium Chemistry," (ACS Symp. Ser. no. 216), edited by W. T. Carnall and G. R. Choppin, (American Chemical Society, Washington, D.C., 1983), p. 173.
- [15] W. T. Carnall and H. M. Crosswhite, "Optical Spectra and Electronic Structure of Actinides Ions in Compounds and in Solution," Argonne National Lab Report ANL-84-90, (1985).
- [16] W. Kot, N. Edelstein, M. M. Abraham, C. B. Finch and L. A. Boatner, unpublished result.
- [17] B. R. Judd and H. Crosswhite, J. Opt. Soc. Am. B 1, 255 (1984).
- [18] L. R. Morss, C. W. Williams and W. T. Carnall in reference 14, p. 206.
- [19] H. M. Crosswhite and H. Crosswhite, J. Opt. Soc. Am. B 1, 246 (1984).
- [20] W. T. Carnall and H. M. Crosswhite in "The Chemistry of the Actinide Elements," Vol. 2, Eds. J. J. Katz, G. T. Seaborg and L. R. Morss, (Chapman and Hall, London, 1986).
- [21] F. Auzel and O. L. Malta, J. Phys. (Paris) 44, 201 (1983).

Table I. Selection Rules for  $f^n$  ( $n = \text{even}$ ) in  $D_{2d}$  Symmetry

Electric Dipole						Magnetic Dipole					
	$\Gamma_1$	$\Gamma_2$	$\Gamma_3$	$\Gamma_4$	$\Gamma_5$		$\Gamma_1$	$\Gamma_2$	$\Gamma_3$	$\Gamma_4$	$\Gamma_5$
$\Gamma_1$				$\pi$	$\sigma$	$\Gamma_1$		$\sigma$			$\pi$
$\Gamma_2$			$\pi$		$\sigma$	$\Gamma_2$	$\sigma$				$\pi$
$\Gamma_3$		$\pi$			$\sigma$	$\Gamma_3$				$\sigma$	$\pi$
$\Gamma_4$	$\pi$				$\sigma$	$\Gamma_4$			$\sigma$		$\pi$
$\Gamma_5$	$\sigma$	$\sigma$	$\sigma$	$\sigma$	$\pi$	$\Gamma_5$	$\pi$	$\pi$	$\pi$	$\pi$	$\sigma$

Table II. Absorption Spectra of  $\text{ZrSiO}_4:\text{Pu}^{4+}$ .<sup>a</sup>

Wavelength (Å)	Energy ( $\text{cm}^{-1}$ )	Polarization	Intensity	Assignment
21690	4608	$\sigma$	W(dis. at 4K)	$\Gamma_5 \rightarrow \Gamma_2$
20150	4960	$\sigma$	W(dis. at 4K)	
20100	4974	$\pi$	VW(dis. at 4K)	
19598	5101	$\pi$	sh	
19492	5129	$\pi$	S	$\Gamma_2$
19280	5185	$\sigma$	VW(dis. at 4K)	
19080	5237	$\pi$	VW, Br	
18822	5311	$\sigma$	sh	
18700	5346	$\sigma, \pi$ VW	VS	$\Gamma_5$
18285	5467	$\sigma$	M	$\text{Pu}(3+)$
18200	5493	$\pi$	VW	
18113	5519	$\sigma$	W	
17912	5581	$\sigma$	W	
17796	5618	$\sigma$	W, sh	
17595	5682	$\pi$	M	
17490	5716	$\sigma, \pi$ VW	M	$\Gamma_5$
17415	5831	$\sigma$	sh	
16963	5894	$\sigma$	M	$\Gamma_5$
16877	5924	$\pi$	VS	$\Gamma_2$
16657	6002	$\sigma$	VW	
15421	6483	$\sigma, \pi$	VW	
15248	6556	$\sigma, \pi$	VW	
11828	8452	$\pi$	W(dis. at 4K)	$\Gamma_5 \rightarrow \Gamma_5$
11450	8731	$\sigma$	VW	$\text{Pu}(3+)$
11400	8769	$\sigma$	VW	$\text{Pu}(3+)$
11341	8816	$\sigma$	VW	$\text{Pu}(3+)$
11151	8966	$\sigma$	sh	$\text{Pu}(3+)$
11140	8974	$\sigma, \pi$ VW	VS	$\Gamma_5$
10895	9176	$\sigma, \pi$	W	$\text{Pu}(3+)$
10730	9317	$\sigma$	VW	
10680	9360	$\pi$	S	
10600	9431	$\sigma$	S	$\Gamma_5$
10593	9438	$\pi$	VS	$\Gamma_2$
10426	9589	$\pi$	M	
10410	9603	$\sigma$	M	$\Gamma_5$
10208	9793	$\pi$	W	
10093	9903	$\sigma, \pi$	VW	
9985	10012	$\pi$	VW	

9928	10070	$\sigma, \pi$	VW	
9609	10404	$\pi$	VW	
9308	10740	$\sigma$	W(dis. at 4K)	$\Gamma_5 \rightarrow \Gamma_2$
9203	10831	$\sigma$	VW(dis. at 4K)	
9105	10979	$\pi$	W	
9017	11087	$\sigma$	W	
8876	11264	$\pi$	VS	$\Gamma_2$
8745	11431	$\sigma, \pi$	W	
8627	11588	$\sigma$	S	$\Gamma_5$
8600	11625	$\pi$	VW, Br	
8365	11951	$\sigma, \pi$	VW	
8181	12221	$\pi$	VS	$\Gamma_2$
8109	12329	$\sigma$	VS	$\Gamma_5$
7985	12520	$\pi$	W	$\Gamma_2$
7948	12578	$\sigma$	S, sh	$\Gamma_5$
7875	12695	$\sigma$	VS	$\Gamma_5$
7628	13106	$\pi$	M	$\Gamma_2$
7620	13120	$\sigma$	S	$\Gamma_5$
7530	13277	$\sigma$	W, sh	
7472	13380	$\pi$	W	
7375	13556	$\sigma$	M	$\Gamma_5$
7320	13657	$\pi$	M	$\Gamma_2$
7175	13933	$\sigma$	S	$\Gamma_5$
7134	14014	$\sigma$	M, sh	
7118	14045	$\sigma$	M	
7050	14180	$\sigma$	M, sh	$\Gamma_5$
6800	14702	$\pi$	VS, Br	$\Gamma_2$
6730	14855	$\pi$	S, sh	$\Gamma_2$
6681	14962	$\sigma$	VS	$\Gamma_5$
6658	15015	$\sigma$	VS	$\Gamma_5$
6640	15047	$\pi$	M, sh	
6574	15205	$\sigma$	M, sh	$\Gamma_5$
6320	15818	$\sigma$	M	$\Gamma_5$
6293	15886	$\pi$	W	
6259	15972	$\sigma$	VW	
6249	15998	$\pi$	W	
6244	16010	$\sigma$	W	$\Gamma_5$
6180	16175	$\sigma$	W	$\Gamma_5$
5783	17287	$\pi$	W	
5773	17317	$\pi$	W, sh	
5770	17324	$\pi$	M	$\Gamma_2$
5765	17340	$\sigma$	W	
5764	17342	$\pi$	VW	
5759	17360	$\sigma$	W	
5749	17388	$\sigma$	W	
5746	17399	$\sigma$	W	
5739	17419	$\sigma$	M, Br	$\Gamma_5$

5731	17442	$\sigma$	W	
5668	17638	$\sigma$	VW	
5660	17662	$\sigma$	VW	
5542	18039	$\pi$	W, Br	$\Gamma_2$
5437	18387	$\sigma$	W, Br	$\Gamma_5$
5286	18911	$\sigma$	W, Br	
5259	19011	$\pi$	W, Br	
5251	19037	$\sigma$	M, Br	$\Gamma_5$
5226	19129	$\pi$	M, Br	$\Gamma_2$
5200	19223	$\sigma$	W, Br	$\Gamma_5$
5174	19321	$\sigma$	W	$\Gamma$
5080	19679	$\sigma$	M, Br	$\Gamma_5$
5039	19838	$\pi$	W, Br	$\Gamma_2$
5019	19918	$\sigma$	M, Br	
4931	20275	$\sigma$	M, Br	$\Gamma_5$
4838	20665	$\sigma$	W	
4837	20669	$\pi$	M, Br	$\Gamma_2$
4749	21052	$\sigma$	VW	
4723	21165	$\sigma$	W, sh	
4714	21209	$\sigma$	W, Br	$\Gamma_5$
4712	21216	$\pi$	M, VBr	
4692	21307	$\pi$	W, sh	
4600	21733	$\pi$	M, Br	$\Gamma_2$
4536	22041	$\sigma$	M, sh	$\Gamma_5$
4506	22184	$\sigma$	M, VBr	
4452	22455	$\pi$	M, VBr	
4421	22611	$\sigma$	W	$\Gamma_5$
4409	22675	$\pi$	M, Br	$\Gamma_2$
4218	23700	$\sigma$	W	$\Gamma_5$
4203	23784	$\pi$	M	$\Gamma_2$
4106	24346	$\pi$	W	
4099	24389	$\pi$	M	$\Gamma_2$
4086	24465	$\sigma$	M	$\Gamma_5$
4082	24488	$\pi$	W	
4026	24831	$\pi$	W, VBr	
3980	25118	$\pi$	W, VBr	

---

<sup>a</sup>VS, very strong; S, strong; M, medium; W, weak; VW, very weak; Br, broad; sh, shoulder.

Table III. Calculated parameters of  $\text{ZrSiO}_4:\text{Pu}^{4+}$  ( $\text{cm}^{-1}$ ). (See text).

	A	B
$F^2$	49394(260)	47909(1270)
$F^4$	39495(494)	37217(1571)
$F^6$	30684(344)	29201(1230)
$\alpha$	323(18)	307(24)
$\beta$	-783(78)	-784(88)
$\gamma$	[1200] <sup>a</sup>	1877(448)
$T^2$	[200]	323(138)
$T^3$	[50]	[30]
$T^4$	[100]	[100]
$T^6$	[-300]	[-300]
$T^7$	[400]	[400]
$T^8$	[350]	[350]
$\zeta$	2366(6)	2359(10)
$M^0$	[0.98]	3.85(0.81) <sup>b</sup>
$M^2$	[0.55]	[2.15]
$M^4$	[0.38]	[1.46]
$P^2$	[500]	931(280) <sup>c</sup>
$P^4$	[375]	[698]
$P^6$	[250]	[466]
$B_0^2$	-2125(118)	-2074(118)
$B_0^4$	2799(162)	2877(158)
$B_4^4$	-5085(106)	-5090(105)
$B_0^6$	-4797(136)	-4945(136)
$B_4^6$	1201(131)	1141(130)
$n^d$	53	53
$\sigma^e$	35	33

<sup>a</sup> Values in [ ] are fixed in the fittings.

<sup>b</sup>  $M^0$  was varied with the fixed ratios  $M^2/M^0 = 0.56$  and  $M^4/M^0 = 0.38$ .

<sup>c</sup>  $P^2$  was varied with the fixed ratios  $P^4/P^2 = 0.75$  and  $P^6/P^2 = 0.50$ .

<sup>d</sup>  $n$  is the number of levels.

<sup>e</sup>  $\sigma = (\sum (E_{\text{cal}} - E_{\text{exp}})^2 / (n-p))^{1/2}$  where  $E_{\text{cal}}$  and  $E_{\text{exp}}$  are the calculated and experimental energies and  $p$  is the number of free parameters.

Table IV. Comparison of Parameters of  $\text{ZrSiO}_4:\text{An}^{4+}$  (Units of Parameters =  $\text{cm}^{-1}$ ).

	$\text{U}^{4+}:\text{ZrSiO}_4^{\text{a}}$	$\text{Np}^{4+}:\text{ZrSiO}_4^{\text{b}}$	$\text{Pu}^{4+}:\text{ZrSiO}_4^{\text{c}}$
$F^2$	44258	47479	49394
$F^4$	40293	41455	39495
$F^6$	31287	26528	30684
$\zeta$	1740	2088	2357
$\alpha$	23	39.2	32.3
$\beta$		-610	-783
$\gamma$		[1200]	[1200]
$B_0^2$	-2000	-2537	-2125
$B_0^4$	2000	2304	2799
$B_4^4$	-5125	-5281	-5085
$B_0^6$	-5792	-5065	-4797
$B_4^6$	427	642	1201
$n$	30	31	53
$\sigma$	112	34	35
$F_{\text{cry}}^2/F_{\text{fi}}^2$	0.85	0.87	0.89
$\zeta_{\text{cry}}/\zeta_{\text{fi}}$	0.88	0.93	0.94
$F_{\text{cry}}^4/F_{\text{cry}}^2$	0.91	0.87	0.80
$N_{\text{v}}(4\pi)^{-1/2}$	3113	3179	3084

<sup>a</sup>Reference 3.<sup>b</sup>Reference 4.<sup>c</sup>This work.



Table V. Comparison of Relativistic Hartree-Fock and Experimental Free Ion Parameters ( $\text{cm}^{-1}$ ).

Parameters <sup>a</sup>	U <sup>4+</sup>	Np <sup>4+</sup>	Pu <sup>4+(b)</sup>
$\Delta F^2$	32466	32413	33514
$\Delta F^4$	9906	10875	14861
$\Delta F^6$	5573	11924	9281
$\Delta\zeta$	370	309	340

<sup>a</sup>  $\Delta F^k = F^k(\text{calc.}) - F^k(\text{exp.})$ ,  $F^k(\text{calc.})$  from reference 15.

<sup>b</sup> Parameter set A from Table III used for Pu<sup>4+</sup>.

Supplementary Table. Observed and Calculated Energies for  $\text{Pu}^{4+}$  in  $\text{ZrSiO}_4$ .

(Parameter Set B, See Text.)

$\Gamma$	Energy ( $\text{cm}^{-1}$ )		$\Delta E$ ( $\text{cm}^{-1}$ )	Eigenvector $(2S+1)L(J, J_z)$	
	calc.	obs.		% largest	% second
3	0	0	0	77	$5I(4, \pm 2)^a$
5	542.8	522.0	20.8	42	$5I(4, -3)$ 31 $5I(4, 1)$
1	706.5			73	$5I(4, \pm 4)$
2	782.0			77	$5I(4, \pm 4)$
4	1097.4			77	$5I(4, \pm 2)$
5	1577.5			44	$5I(4, 1)$ 32 $5I(4, -3)$
1	1738.8			71	$5I(4, 0)$ 9 $3H_4(4, 0)$
2	5140.5	5129.0	11.5	66	$5I(5, \pm 4)$
1	5213.0			80	$5I(5, \pm 4)$
5	5336.6	5346.0	-9.4	65	$5I(5, 5)$ 17 $5I(5, 1)$
5	5689.4	5716.0	-26.6	38	$5I(5, 1)$ 27 $5I(5, -3)$
4	5758.6			84	$5I(5, \pm 2)$
5	5850.5	5894.0	-43.5	56	$5I(5, -3)$ 22 $5I(5, 1)$
2	5957.8	5924.0	23.8	67	$5I(5, 0)$ 10 $5I(5, 4)$
3	5991.5			85	$5I(5, \pm 2)$
4	8255.0			25	$5I(6, \pm 6)$
1	8719.8			24	$5F(2, 0)$ 13 $5G(2, 0)$
5	8948.9	8974.0	-25.1	58	$5I(6, 5)$ 11 $5I(6, 1)$
3	9136.0			71	$5I(6, \pm 6)$
1	9404.5			38	$5I(6, 0)$ 22 $5I(6, 4)$
5	9415.4	9431.0	-15.6	43	$5I(6, 1)$ 9 $5F(2, 1)$
2	9445.7	9438.0	7.7	76	$5I(6, \pm 4)$
4	9460.9			52	$5I(6 \pm 2)$
3	9518.4			72	$5I(6 \pm 2)$
5	9663.5	9603.0	60.5	56	$5I(6, -3)$ 11 $5I(6, 1)$

1	9863.5			40	5I(6,0)	17	5I(6,4)
4	9955.7			35	5I(6,±6)		
5	9989.1			19	5I(6,-3)	13	5I(6,5)
3	10908.8			23	5F(2,±2)		
2	11276.5	11264.0	12.5	62	5F(1,0)	11	3D1(1,0)
5	11581.9	11588.0	-6.1	22	5I(7,-7)	16	5F(1,1)
5	11689.0			31	5F(1,1)	6	3D1(1,1)
1	11985.6			11	3G2(4,±4)		
3	12051.3			10	5I(7,±6)		
5	12106.2			22	5I(7,-3)	22	5F(1,1)
2	12200.9	12221.0	-20.1	5	3G2(4,-4)	5	5F(1,0)
5	12314.1	12329.0	-14.9	39	5I(7,5)	12	5I(7,1)
4	12388.6			38	5I(7,±2)		
3	12444.6			23	5I(7,±6)		
2	12484.8	12520.0	-35.2	47	5I(7,±4)		
1	12523.9			56	5I(7,±4)		
5	12552.7	12578.0	-25.3	24	5I(7,-3)	15	5I(7,-7)
4	12574.5			35	5I(7,±6)		
3	12703.7			19	5I(7,±6)		
5	12740.7	12695.0	45.7	26	5I(7,1)	14	5I(7,5)
4	13086.6			14	5F(2,±2)		
2	13124.8	13106.0	18.8	51	5I(7,0)	12	3K2(7,0)
5	13136.6	13120.0	16.6	21	5I(7,1)	7	5F(4,1)
1	13187.6			12	5F(4,0)	11	3G2(4,0)
3	13236.3			31	5G(2,±2)		
5	13607.1	13556.0	51.1	17	5G(3,-3)	11	5S(2,1)
4	13655.0			27	5G(2,±2)		
2	13669.3	13657.0	12.3	59	5F(3,0)	7	3F3(3,0)
3	13773.4			35	5F(3,±2)		
4	13912.5			25	5G(3,±2)		
5	13925.7	13933.0	-7.3	51	5F(3,1)	7	3F3(3,1)
1	14020.4			36	5G(2,0)	19	5F(2,0)
5	14172.4	14180.0	-7.6	24	5F(3,-3)	11	5G(2,1)
4	14684.6			17	5S(2,±2)		

2	14705.0	14702.0	3.0	52	5G(3,0)	7	3G2(3,0)
1	14727.9			27	5I(8,±4)		
3	14799.4			18	5F(3,±2)		
5	14829.7			19	5I(8,-3)	9	3K2(8,-3)
2	14853.6	14855.0	-1.4	34	5I(8,±4)		
3	14882.4			32	5I(8,±2)		
1	14886.1			38	5S(2,0)	15	3P2(2,0)
5	14894.7	14962.0	-67.3	30	5I(8,5)	14	3K2(8,5)
5	15024.7	15015.0	9.7	12	5S(2,1)	10	5I(8,5)
5	15170.3	15205.0	-34.7	41	5G(3,1)	12	3G2(3,1)
2	15180.0			31	5I(8,±8)		
4	15287.2			37	5I(8,±6)		
1	15290.1			30	5I(8,±8)		
3	15402.5			39	5I(8,±6)		
4	15797.2			25	5S(2,±2)		
5	15843.6	15818.0	25.6	39	5I(8,-7)	21	3K2(8,-7)
5	16041.3	16010.0	31.3	14	5G(3,-3)	10	5I(8,-3)
4	16123.2			26	5I(8,±2)		
1	16123.9			26	5I(8,0)	17	3K2(8,0)
5	16137.0	16175.0	-38.0	18	5S(2,1)	14	5I(8,1)
3	16158.1			27	5S(2,±2)		
2	17373.3	17324.0	49.3	22	5F(5,±4)		
5	17394.7	17419.0	-24.3	19	5F(5,-3)	10	5F(5,1)
4	17398.4			20	5F(5,±2)		
1	17553.4			10	5F(4,0)	9	5F(5,-4)
1	17741.9			31	5F(4,0)	10	5G(4,0)
5	17788.1			38	5F(4,1)	13	5G(4,1)
4	17932.2			14	3K2(6,±6)		
5	17986.2			19	3K2(6,5)	9	5F(5,5)
3	17997.6			23	3K2(6,±6)		
1	18041.0			28	3K2(6,0)	9	3K1(6,0)
2	18061.6	18039.0	22.6	11	5F(5,0)	9	3K2(6,4)
5	18157.8			39	3K2(6,1)	14	3K1(6,1)

3	18342.0			23	3K2(6,±2)		
5	18384.3	18387.0	-2.7	30	3K2(6,-3)	13	3K2(6,5)
4	18408.6			29	5F(4,±2)		
1	18413.2			32	3K2(6,±4)		
4	18440.5			30	3K2(6,±2)		
5	18446.3			12	3K2(6,-3)	8	5F(5,5)
3	18455.8			18	3K2(6,±6)		
2	18487.5			27	3K2(6,±4)		
5	18612.1			21	5F(4,-3)	9	5F(5,1)
3	18946.8			27	5F(4,±2)		
1	18962.1			32	5F(4,±4)		
5	19019.6	19036.9	-17.3	16	3L(7,-7)	15	3L(7,-3)
3	19086.4			37	3L(7,±2)		
2	19110.5	19128.5	-18.0	21	5F(4,±4)		
5	19180.8	19223.0	-42.2	17	3L(7,-3)	14	5F(4,-3)
5	19282.2	19321.0	-38.8	18	3L(7,-7)	12	5F(4,-3)
2	19309.9			20	3L(7,0)	10	5I(7,0)
1	19493.0			35	3L(7,±4)		
4	19529.4			32	3L(7,±2)		
5	19663.8	19679.0	-15.2	26	3L(7,1)	12	5I(7,1)
2	19894.5	19838.0	56.5	16	3L(7,0)	8	3L(7,-4)
5	20055.7			33	3L(7,5)	14	5I(7,5)
3	20189.3			32	3L(7,±6)		
1	20226.1			14	5F(2,0)	9	5I(8,0)
4	20299.5			36	3L(7,±6)		
5	20306.8	20275.0	31.8	44	5G(4,-3)	5	3H4(4,-3)
1	20412.7			18	5G(4,0)	9	5G(4,-4)
4	20589.8			15	5F(2,±2)		
2	20635.0	20669.0	-34.0	39	5G(4,±4)		
5	20731.5			13	3M(8,1)	12	5G(4,1)
3	20801.2			29	5G(4,±2)		
3	21043.9			22	3M(8,±2)		
1	21109.2			8	3M(8,4)	8	5D(0,0)

4	21169.9			25	3M(8,±2)		
5	21203.3	21208.8	-5.5	15	3M(8,5)	12	5G(5,1)
5	21313.1			9	3M(8,1)	9	3M(8,-3)
2	21356.8			32	5G(5,0)	25	5F(5,0)
1	21402.1			38	5D(0,0)	11	3P1(0,0)
2	21479.5			16	5G(5,±4)		
5	21540.7			21	5F(5,1)	12	5G(5,1)
5	21609.0			14	3M(8,-7)	8	5I(8,-7)
3	21695.5			20	5G(5,±2)		
1	21737.4			17	3M(8,0)	11	5I(8,0)
2	21745.4	21733.0	12.4	11	3G2(3,0)	8	3M(8,4)
4	21817.7			15	3M(8,±6)		
5	21919.6			9	3M(8,-7)	7	5I(8,-7)
1	22019.6			22	3M(8,±8)		
5	22053.2	22041.4	11.8	9	5F(5,-3)	8	3G2(3,1)
4	22109.2			9	5F(5,±2)		
3	22110.5			20	5F(2,±2)		
4	22241.7			21	3G2(3,±2)		
2	22249.3			29	5F(5,±4)		
5	22339.2			7	3D1(2,1)	7	5S(2,1)
5	22388.8			11	3G2(3,-3)	8	3G2(3,1)
1	22396.3			12	5G(5,±4)		
1	22558.6			22	5F(5,±4)		
5	22605.6	22610.8	-5.2	27	5F(5,5)	10	5G(5,5)
3	22641.0			25	3G2(3,±2)		
2	22675.9	22675.0	0.9	15	3G2(3,0)	7	3G3(3,0)
5	22857.6			20	5F(5,-3)	7	5G(4,1)
3	22895.5			19	3D1(2,±2)		
4	23025.9			20	5F(5,±2)		
2	23070.3			28	5D(1,0)	11	3P2(1,0)
5	23336.6			16	5D(1,1)	8	3P2(1,1)
4	23531.5			11	1D3(2,±2)		
5	23693.0	23699.7	-6.7	9	3F3(2,1)	9	3P2(1,1)
2	23770.0	23784.0	-14.0	19	3P2(1,0)	17	5D(1,0)

1	23901.5			12	1D3(2,0)	11	3F3(2,0)
3	24073.7			14	1D3(2,±2)		
4	24222.8			31	5G(6,±2)		
5	24267.8			17	5G(6,1)	14	5D(1,1)
5	24334.7			9	5G(6,-3)	8	5D(1,1)
1	24377.6			14	3I1(5,±4)		
3	24382.4			21	3F4(4,±2)		
2	24441.2	24398.0	52.2	15	5G(5,±4)		
5	24456.1	24465.1	-9.0	11	3F4(4,1)	8	5D(4,1)

---

<sup>a</sup>Contributions from  $+J_z$  and  $-J_z$  are equal and have been summed.

*LAWRENCE BERKELEY LABORATORY  
TECHNICAL INFORMATION DEPARTMENT  
UNIVERSITY OF CALIFORNIA  
BERKELEY, CALIFORNIA 94720*